Chapter 8
Multiparametric MRI of the Prostate as a Tool for Prostate Cancer Detection, Localization, and Risk Assessment

Marc A. Bjurlin, Neil Mendhiratta, and Samir S. Taneja

Introduction

Advances in multiparametric magnetic resonance imaging (mpMRI) hold promise for the improved detection and characterization of prostate cancer [1]. MpMRI combines diffusion-weighted imaging, dynamic contrast-enhanced sequences, or spectroscopy with conventional T2-weighted sequences. With a combination of anatomic and functional imaging sequences to identify suspicious regions in the prostate, pre-biopsy mpMRI has the potential to improve prostate cancer detection and risk stratification through MRI-targeted biopsy [2]. In this chapter we review the role of mpMRI in prostate cancer detection, the outcomes of MRI-targeted biopsy, and the critical concepts currently under evaluation in validation of an MRI-based prostate cancer risk stratification strategy.

Limitations of Contemporary Systematic Biopsy Technique and Methods for Prostate Cancer Detection

The contemporary random 12-core systematic biopsy strategy relies on sampling efficiency for cancer detection and is consequently subject to sampling error. Cancers are often small, intermingled with benign stroma, and not uniformly distributed

M.A. Bjurlin, D.O. • S.S. Taneja, M.D. (✉)
Division of Urologic Oncology, Department of Urology, NYU Langone Medical Center, 150 E 32nd Street, 2nd Floor, New York, NY 10016, USA
e-mail: marc.bjurlin@gmail.com; samir.taneja@nyumc.org

N. Mendhiratta, B.A.
School of Medicine, NYU Langone Medical Center, 550 1st Avenue, New York, NY 10016, USA
e-mail: Neil.Mendhiratta@nyumc.org

N.N. Stone, E.D. Crawford (eds.), *The Prostate Cancer Dilemma*,
DOI 10.1007/978-3-319-21485-6_8

within the gland. As a result, clinically significant cancers frequently go undetected. Under-sampling of the prostate during ultrasound-guided biopsy also leads to incorrect risk stratification in a subset of men with a potential for categorization of clinically significant tumors as low volume or low grade. Random non-targeted prostate biopsies risk inadequate sampling of a cancer lesion often at its periphery. This may reveal a small length of tumor in a core with a low Gleason score, when in fact a clinically significant lesion may exist adjacent to the biopsy site. Approximately 30–50 % of men over age 50 years harbor clinically insignificant PCa at autopsy. These clinically insignificant cancers are often identified by chance during a systematic biopsy approach, contributing, in part, to the problem of over-detection and over-treatment of indolent PCa. Repeat biopsy increases detection of clinically insignificant PCa. The recent trend of overcoming sampling error through increasing core number, or repeating biopsies, further escalates the risk of identifying small, indolent cancers which may have little to do with the patient's PSA elevation [3].

Introducing pre-biopsy mpMRI and MRI-targeted biopsy in the evaluation of men at risk for prostate cancer has the potential to address many of the shortcomings of contemporary clinical approaches to prostate cancer diagnosis using systematic biopsy. Potential advantages of pre-biopsy mpMRI and MRI-targeted biopsy include increased detection of high-risk prostate cancer, reduced detection of low risk, indolent disease, utilization of fewer biopsy cores, reduction of the number of men needing biopsy, and better sampling of cancer leading to more accurate risk stratification [4, 5].

Multiparametric MRI: Image Sequences

T2-Weighted Imaging

T2-weighted MR images, reflecting tissue water content, have high spatial resolution and clearly define the prostate's zonal anatomy, distinguishing the peripheral zone (high signal intensity) from the central zone (surrounding the ejaculatory ducts in the posterior prostate base and exhibiting decreased T2 signal intensity) and transition zones (surrounding the urethra, extending anteriorly and superiorly from the level of the verumontanum, and exhibiting heterogeneous, often swirled, signal intensity) (Fig. 8.1) [6]. In the peripheral zone, PCa can appear as an area of low signal intensity. The degree of intensity decrease differs with the Gleason score, with higher Gleason score components showing lower signal intensities [7]. T2-weighted imaging results in false-positive findings, as low signal intensity can also be the consequence of benign abnormalities including acute and chronic prostatitis, atrophy, scars, post-irradiation or hormonal treatment effects, hyperplasia, and post-biopsy hemorrhage. Partly related to the heterogeneous appearance of BPH with areas of both increased and decreased signal intensity, cancer in transition zone may be more difficult to discern than in the peripheral zone, particularly for the less experienced radiologist. However, morphological features such as homogeneously low signal

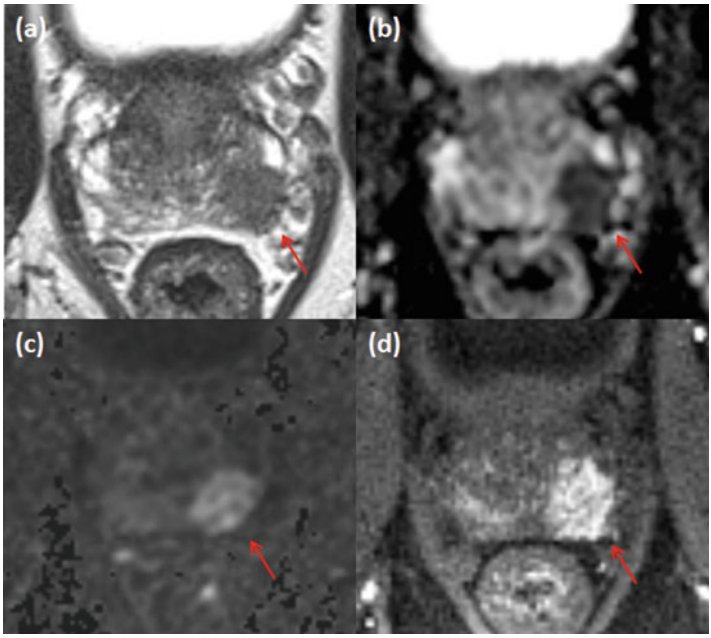

Fig. 8.1 Sixty-six year-old biopsy naïve male with a PSA of 6.2 underwent mpMRI demonstrating a Likert scale suspicion score of 5/5 in the left posterolateral base to mid peripheral zone lesion: T2WI (**a**), ADC (**b**), DWI (*b*-value 1500) (**c**), and DCE (single time-point (**d**)). Systematic biopsy demonstrated Gleason score 6 (3+3) prostate cancer while MRI-targeted biopsy demonstrated Gleason score 8 (4+4) cancer in 4/4 cores. *Red arrow* points to lesion

intensity, ill-defined irregular edges of the suspicious lesion, invasion into the urethra or the anterior fibromuscular stroma, and lenticular shape are helpful for detection of transition zone tumor [8].

Diffusion-Weighted Imaging

Diffusion-weighted (DW) MRI measures random motion of water molecules. The strength of the gradient that determines the degree of diffusion-weighting is reflected by the sequence's *b*-value. By performing DWI with multiple *b*-values, it is possible to compute the apparent diffusion coefficient (ADC) based on the signal intensity measured at each *b*-value image to quantify the restriction of water diffusion (Fig. 8.1). Traditionally, a maximal *b*-value of around 1000 s/mm^2 has been used. More recent data show that use of higher *b*-values up to 2000 s/mm^2 helps eliminate background signal from normal prostate and may increase the accuracy of PCa detection [9], within both the peripheral zone and transition zone [10]. However, modern MRI hardware and careful attention to sequence optimization is required to

maintain image quality when using these very high *b*-values. On ADC maps, PCa frequently shows low ADC [11], and an inverse correlation exists between quantitative ADC values and the Gleason score [12]. While ADC does correlate with final Gleason score, the confidence intervals are widely overlapping, limiting the ability to use ADC as a surrogate of Gleason score. This is an area of ongoing investigation and technical optimization aimed to improve ADC's predictive ability in the future. Limitations of DWI include low signal-to-noise ratio and image distortion, both of which become more problematic at higher *b*-values. Nonetheless, DWI is a widely available technique with relatively straightforward acquisition and post-processing. Moreover, given its strong association with tumor aggressiveness, it may prove to be the primary sequence for tumor detection and characterization [13].

Perfusion Imaging

Dynamic contrast-enhanced (DCE) MRI consists of a series of fast T1-weighted sequences covering the prostate before and after rapid injection (2–4 mL/s) of a bolus of a gadolinium chelate. Given the serial rapid imaging of the prostate, DCE-MRI allows assessment of contrast kinetics within focal lesions (Fig. 8.1). PCa typically enhances faster and to a greater extent than surrounding prostate, and will also show more rapid washout of contrast in a fraction of cases. Even though prostatitis-related enhancement is usually diffuse and non-focal in nature, and BPH-related enhancement is often well-encapsulated and spherical, the non-specific nature of these patterns limits the utility of DCE findings in isolation, resulting in DCE often being applied largely as an adjunct to interpretations based primarily on findings on T2WI and DWI. A simple approach to evaluating DCE-MRI is through a subjective visual assessment of the raw dynamic images. Alternatively, semi-quantitative parameters, such as the time-to-peak, wash-in rate, and washout rate, may be computed to allow pixel-wide construction of parametric perfusion maps. A compartment-based model may also be performed to generate truly quantitative metrics. This has largely been performed using a Tofts model, which provides the parameter k^{trans} (transfer constant), reflecting the forward transfer rate constant between the plasma and extravascular extracellular space and is elevated in PCa [14].

One limitation of DCE-MR imaging relates to overlap of cancer with prostatitis in the peripheral zone and marked overlap with vascularized BPH nodules in the transition zone. Another limitation is the reduced spatial resolution due to fast imaging.

Accuracy in Detection/Performance Characteristics

While these individual sequences all have utility in PCa detection, results are optimized by multiparametric (mp) MRI, combining all of the sequences in an integrated fashion (Fig. 8.1). MpMRI offers superior diagnostic power for PCa detection

and can assist risk stratification based on lesion size, extent, and ADC value [15]. In one study, mpMRI sensitivity exceeded 80 % for detecting 0.2 cm^3 of Gleason 4 + 3 or above and 0.5 cm^3 of ≥Gleason 3 + 4 [16]. In another study using a 3 T magnet, addition of DCE and/or DW imaging to T2-weighted MRI significantly improved sensitivity from 63 % to 79–81 % in the peripheral zone, while maintaining a stable specificity [17]. Yoshizako et al. demonstrated the combined use of DW, DCE, and T2-weighted MRI to increase accuracy in detection of transition zone cancer compared to T2WI alone, from 64 to 79 % [18]. Nevertheless, given moderate specificity, mpMRI findings require biopsy to confirm the presence of tumor and assess Gleason score [15]. PCa MRI suspicion scores have been developed for improved standardization of MRI interpretation and reporting [19, 20].

MRI Suspicion Score

Prostatic abnormalities, often termed regions of suspicion, identified on mpMRI have the potential to localize high-risk prostate cancer. Lesions are commonly scored on a Likert scale as 2 (low probability), 3 (equivocal), 4 (high probability), or 5 (very high probability), or the standard-based Prostate Imaging-Reporting and Data System (PI-RADS) as I (very low), II (low), III (indeterminate), IV (high), V (very high), as previously described [21–23]. The performance characteristics of MRI suspicion score in predicting the likelihood of cancer are highly interpreter-dependent. Individual institutional variation in reporting of Likert scales of suspicion results in variability in cancer detection rates observed on biopsy. This serves as a primary impetus for the implementation of a standardized reporting scheme such as PI-RADS. Most recently in version 2 of PI-RADS (Tables 8.1 and 8.2), the standardized scheme has been greatly simplified [23].

MRI suspicion score strongly predicts the likelihood of cancer on MRI-targeted biopsy. In a study of 105 subjects with prior negative biopsy and elevated PSA values who underwent mpMRI targeted biopsy, a highly suspicious MRI abnormality was the most significant predictor of significant cancer on multivariate analysis [24]. Yerram et al. evaluated 125 patients with only low suspicion prostatic lesions on mpMRI and determined these lesions are associated with either negative biopsies or low-grade tumors suitable for active surveillance [25]. Our institution has also reported a positive trend between increasing suspicion score on mpMRI and detection of high-grade (GS ≥ 7 PCa) disease, but not with detection of Gleason score 6 cancer [5].

Negative Predictive Value of MRI

One potential benefit of the utilization of pre-biopsy MRI in clinical practice would be the opportunity to reduce biopsy utilization among men at risk. A growing body of literature has begun to address the negative predictive value (NPV) of MRI in

Table 8.1 PI-RADS 2.0 mpMRI interpretation

Score	T2W (PZ)	T2W (TZ)	DWI (PZ and TZ)	Score	DCE (PZ and TZ)
1	Uniform hyperintense signal intensity	Homogenous intermediate signal intensity	No abnormality on ADC and high *b*-value DWI	(−)	No early enhancement, or Diffuse enhancement not corresponding to a focal finding on T2 and/or DWI or Focal enhancement corresponding to a lesion demonstrating features of BPH on T2WI
2	Linear/wedge-shaped hypointensity or diffuse mild hypointensity	Circumscribed hypointense or heterogenous encapsulated nodules	Indistinct hypointense on ADC		
3	Heterogenous signal intensity or non-circumscribed, rounded, moderate hypointensity	Heterogenous signal intensity with obscured margins	Focal mildly/moderately hypointense on ADC and isointense/mildly hyperintense on high *b*-value DWI		
4	Circumscribed, homogenous moderate hypointense focus/mass confined to prostate and <1.5 cm in greatest dimension	Lenticular or non-circumscribed, homogenous, moderately hypointense, and <1.5 cm in greatest dimension	Focal markedly hypointense on ADC and markedly hyperintense on high *b*-value DWI; <1.5 cm in greatest dimension	(+)	Focal, and; Earlier than or contemporaneously with enhancement of adjacent normal prostatic tissues, and; Corresponds to suspicious finding on T2W and/or DWI
5	Same as 4 but ≥1.5 cm in greatest dimension or definite extraprostatic extension/invasive behavior	Same as 4 but ≥1.5 cm in greatest dimension or definite extraprostatic extension/invasive behavior	Same as 4 but ≥1.5 cm in greatest dimension or definite extraprostatic extension/invasive behavior		

Adapted from Radiology ACo. MR Prostate Imaging Reporting and Data System version 2.0. 2015; http://www.acr.org/Quality-Safety/Resources/PIRADS/, (2015).

Table 8.2 PI-RADS 2.0 scoring rubric

	Peripheral zone			Transition zone		
Score	DWI	T2W	DCE	DWI	T2W	DCE
1	1	Any	Any	Any	1	Any
2	2	Any	Any	Any	2	Any
3	3	Any	(−)	≤4	3	Any
4	3	Any	(+)	5	3	Any
	4	Any	Any	Any	4	Any
5	5	Any	Any	Any	5	Any

Adapted from Radiology ACo. MR Prostate Imaging Reporting and Data System version 2.0. 2015; http://www.acr.org/Quality-Safety/Resources/PIRADS/, (2015).

ruling out cancer in men for whom there is clinical suspicion. A normal or low suspicion MRI has the potential to allow men to avoid an unnecessary prostate biopsy, and secondarily to reduce the over-detection of indolent disease.

Kumar et al. evaluated 36 men who had a PSA between 4 and 10 ng/mL and a magnetic resonance spectroscopic image (MRSI) that did not show any malignant voxels [26]. Of the 26 men who met follow-up criteria, an initial MRSI negative for a lesion suspicious for malignancy maintained a high negative predictive value (96.2 %), even after an average period of more than 2 years. The authors concluded that a prostate biopsy can be deferred in patients with an increased serum PSA of 4–10 ng/mL and a negative MRSI. Squillaci et al. reported on suspicious lesion on transrectal ultrasound that was further evaluated by mpMRI with proton MR spectroscopy (MRSI). This study reported a NPV for overall cancer detection of T2W-MRI alone, MRSI alone, and combined MRI/MRSI as 69 %, 91 %, and 74 %, respectively [27]. Manenti et al. also showed the prostate biopsy results of 39 men undergoing mpMRI with MRSI, reporting a similar NPV of T2W-MRI, MRSI, and combined MRI/MRSI of 77 %, 74 %, and 74 %, respectively [28].

Although the NPV of mpMRI is high in terms of overall cancer detection rates (CDR), a paucity of data exists on the NPV of mpMRI for clinically significant prostate cancer. In our institutional experience we evaluated 75 men presenting for prostate biopsy who underwent pre-biopsy mpMRI that was negative for suspicious foci, defined as a MRI suspicion score of 1/5 as previously described [21]. Overall, cancer was detected in 14 (18.7 %) men [29]. One (1.3 %) was found to have Gleason 3+4 and the remaining 13 (17.3 %) were found to have Gleason sum 6 (GS6). No Gleason sum ≥ 7 (GS ≥ 7) were detected in men without prior biopsy or on active surveillance. Overall, the NPV for detecting any cancer on systematic 12-core biopsy for men with a negative MRI was 81.3 % and 98.7 % for detecting GS ≥ 7. These NPV were 86.2 % and 100 % for men without prior biopsy, 88.0 % and 96 % for men with a prior negative biopsy, and 61.9 % and 100 % for men on active surveillance. On multivariate analysis, no prior biopsy and a prior negative biopsy were significantly associated with decreased cancer detection on systematic prostate biopsy with a negative mpMRI.

In a recent prospective trial of 226 men who had 3 T mpMRI prior to primary biopsy, Pokorny et al. reported negative biopsies in 56/81 (69 %) men with normal mpMRI [30]. However, this group included men with both PIRADS 1 and 2 mpMRI scores. Among the 25 men with normal mpMRI and prostate cancer on biopsy, 80 % had low-risk disease (low volume Gleason score 3+3 or very low volume Gleason score 3+4), making the NPV for intermediate/high risk disease 94 %. The authors highlight that mpMRI with MRI targeted prostate biopsy reduces the detection of low-risk prostate cancer and reduces the number of men requiring biopsy while improving the overall rate of detection of intermediate/high-risk prostate cancer, a conclusion that is supported by several additional studies [31, 32].

These findings, taken together, lend further support to the utility of mpMRI in predicting negative biopsy among men with clinical suspicion for prostate cancer. The performance characteristics of mpMRI appear to have a high clinical NPV where mpMRI may ultimately be a useful tool to rule out clinically significant prostate cancer on initial evaluation, therefore avoiding unnecessarily prostate biopsies. Validation of this concept will require standardized prospective study.

Correlation of MRI with Surgical Pathology: Disease Localization

There is strong evidence that mpMRI accurately localizes prostate cancer foci larger than 0.2 mL and/or high-grade disease [30, 33]. Accurate identification of index tumor location on mpMRI, followed by fusion of the MR image with a transrectal ultrasound image, could potentially guide targeted biopsy of such index tumors with greater accuracy. Moreover, for image-guided focal therapy, imaging must be able to guide therapy and accurately define margins of the tumor to allow accurate treatment and follow-up. The findings of mpMRI have been compared with whole mount radical prostatectomy specimens and have been evaluated to address the concordance of the index tumor location and the index tumor volume.

In initial studies comparing MRI with whole mount radical prostatectomy specimens to determine tumor site and size concordance, Villers et al. assessed the value of pelvic phased array DCE MRI for predicting the intraprostatic location and volume of clinically localized prostate cancers [16]. Sensitivity, specificity, and positive and negative predictive values for cancer detection by magnetic resonance imaging were 77 %, 91 %, 86 % and 85 % for foci greater than 0.2 cc, and 90 %, 88 %, 77 % and 95 % for foci greater than 0.5 cc, respectively. Kim et al. [34] and Nakashima et al. [35] observed similar performance characteristics of MRI in determining cancer foci location and size. More recent studies which have incorporated modern multiparametric sequences have shown that mpMRI has >90 % specificity in detecting index tumors [36, 37]. In a multi-institutional study of 135 men who had pre-biopsy MRI, MR-TRUS image-fusion biopsy, and robotic radical prostatectomy, followed by whole mount step section of the specimen, MR-TRUS fusion biopsy accurately identified the location of the index tumor in

95 % of patients. In the remaining 5 % of patients, the index tumor was invisible on MRI; each of these tumors was very small (histological tumor volume ≤0.4 mL for radical prostatectomy specimens). These data suggest that MR-TRUS image-fusion biopsies could become a valuable tool in identifying the location of clinically important prostate cancer. However, not all prostate cancer lesions are detectable on MRI, even when using advanced technology. The MRI visibility of prostate cancer depends on cancer volume, grade, histology, and location in comparison to the histological architecture of normal adjacent prostate tissue.

Determining tumor volume concordance, rather than the index lesions site, appears to be a more challenging undertaking with varied success. In a series of 75 men, Isebaert et al. correlated mpMRI and histopathological tumor volumes after radical prostatectomy [38]. Tumor volume was found to be the most accurately assessed by means of DW MRI ($r=0.75$). In a retrospective analysis of 135 men, Baco et al. determined a coefficient for correlation between index lesion volume on MRI and histology was $r=0.663$ [39]. The authors acknowledge the absence of significant agreement between the two and additional MRI variables are necessary to improve tumor volume estimations. Turkbey et al. evaluated 135 patients who underwent multiparametric 3 T endorectal coil magnetic resonance imaging of the prostate and subsequent radical prostatectomy [37]. They observed a positive correlation between histopathology tumor volume and MRI tumor volume (Pearson coefficient 0.633). MRI accurately estimated the index tumor volume independent of Gleason score. MRI had a better accuracy than clinical variables (serum PSA, patient age) in the distinction of tumors larger than 0.5 cm^3.

In our institutional experience, Le Nobin et al. evaluated the level of agreement in volumes of prostate cancer index lesions between histopathology and MRI in 37 men [40]. The authors addressed many of the shortcoming of previous whole mount studies, such as imprecise estimates of pathological volume as the reference standard, suboptimal techniques for achieving co-registration of MRI and pathological images, and the use of correlative statistical methods (such as the Pearson correlation coefficient), by investigating the accuracy of volume estimates from 3 T multiparametric MRI using novel co-registration software. The volume estimates of prostate cancer using MRI tended to substantially underestimate histopathological volumes, with a wide variability in extent of underestimation across cases. Rud et al. similarly compared tumor volume and tumor burden between MRI and histology from radical prostatectomy specimens in 199 men and observed MRI underestimates both tumor volume and tumor burden compared with histology [36]. The rate of detection of the index tumor was 92 %, while the overall rate of detection of tumors with a histology tumor volume of >0.5 mL was 86 %. Cornud et al. studied 84 men who had a mpMRI prior to prostatectomy and analyzed mpMRI and pathological tumor volume [41]. The authors similarly observed a wide variation in overestimation and underestimation of MRI tumor volume compared to pathological volume.

In the context of potential focal ablation, Anwar et al. analyzed mpMRI of 20 men who underwent radical prostatectomy with the aim of defining the contour of treatable intraprostatic tumor foci in prostate cancer [42]. By comparing histopathological tumor maps from whole-mount step sections the authors calculated the

margin of error between imaging and histopathological contours at both capsular and non-capsular surfaces and the treatment margin required to ensure at least 95 % tumor coverage if the patient was to undergo targeted therapy. They concluded mpMRI can be used to accurately contour these tumor foci; complete tumor coverage is achieved by expanding the treatment contour at the non-capsular margin by 5 mm. Our institutional experience has shown that MRI underestimates histologically determined tumor boundaries, especially for high MRI suspicion score and high Gleason score lesions [43]. A 9 mm treatment margin around an MRI-visible lesion consistently ensures treatment of the entire histological tumor volume during focal ablative therapy. In assessing tumor volume and tumor margins, mpMRI tended to underestimate lesion size for high-grade tumors while overestimating the size of low-grade tumors. The latter may relate, in part, to stromal reaction and inflammation in the surrounding tissues.

Outcomes of MRI-Targeted Biopsy in Clinical Practice

There are a number of potential benefits of MRI-targeted biopsy which are reported in the literature; however, these still need to be proven though further studies. In theory, accurate localization of significant cancer prior to biopsy may potentially correct limitations of systematic biopsy. Accurate targeting of biopsy cores should reduce false-negative biopsies and improve accuracy in risk classification through better sampling of tumor, with the intent of detecting high-risk disease and avoiding indolent cancer (Table 8.3). Secondarily, a reduction in false-negative biopsies could reduce the necessity for repeat biopsies, thereby reducing cost. Because targeted biopsy relies upon image guidance, fewer cores potentially would be required, additionally reducing cost. Finally, if metrics can be established to demonstrate the lowest risk parameters for detection of clinically significant disease, avoidance of biopsy among men falling below that threshold may reduce the number of biopsies performed and secondarily reduce over-detection. These principles remain to be fully proven, but there is a growing body of evidence to support the assertion.

Several institutions, including our own, have now accrued a mature dataset highlighting the outcomes of MRI-targeted biopsy. In our institutional experience of 601 men, we also found that MRI-US fusion-targeted biopsy detects more high-grade cancer compared to systematic biopsy while limiting over-detection of indolent disease in all men presenting for prostate biopsy [5]. The National Cancer Institute has shown an increased detection of high-risk prostate cancer and decreased detection of low-risk prostate cancer in their experience of 1003 targeted MR/ultrasound fusion biopsies [4]. Collectively, the published literature suggests that overall cancer detection is decreased by MR-targeted biopsy compared to systematic biopsy, but higher grade cancers are detected with fewer cores, and insignificant cancers are detected less often [24, 44].

Table 8.3 Summary of trials of MRI-ultrasound fusion-targeted biopsy in which the cancer detection rate (CDR) of clinically significant cancer was reported

Investigators	Study size	Biopsy history	MRI field strength and additional sequences[a]	TB technique	SB technique	Definition of clinically significant cancer	Overall CDR (TB)	Overall CDR (SB)	Clinically significant CDR (TB)	Clinically significant CDR (SB)
Mozer et al. [47]	152	100 % BN	1.5 T	Transrectal	12-core TRUS	CCL ≥ 4 mm or GS ≥ 3 + 4	54 %	57 %	43 %	37 %
Sonn et al. [24]	105	100 % PNB	3.0 T	Transrectal	12-core TRUS	CCL ≥ 4 mm or GS ≥ 3 + 4	24 %	28 %	22 %	15 %
Wysock et al. [59]	125	54 % BN 27 % PNB 19 % AS	3.0 T	Transrectal	12-core TRUS	GS ≥ 3 + 4	Cohort: 36 % BN: 40 %	Cohort: NR BN: 55 %	Cohort: 23 % BN: 33 %	Cohort: NR BN: 33 %
Kuru et al. [61]	347	51 % BN 49 % PNB	3.0 T	Transperineal	24-core Transperineal	NCCN criteria (intermediate or high risk)	51 %	50 %	41 %	38 %
Fiard et al. [64]	30	43 % BN 57 % PNB	3.0 T	Transrectal	12-core TRUS	≥10 mm cancer or GS ≥ 3 + 4	55 %	43 %	50 %	33 %
Rastinehad et al. [65]	105	33 % BN 67 % PNB	3.0 T	Transrectal	12-core TRUS	Epstein criteria	51 %	49 %	45 %	32 %
Sonn et al. [66]	171	38 % PNB 62 % AS	3.0 T	Transrectal	12-core TRUS	GS ≥ 3 + 4	35 %	44 %	13 %	12 %
Siddiqui et al. [4]	1003	20 % BN 43 % PNB 37 % AS	3.0 T Spectroscopy	Transrectal	12-core TRUS	GS ≥ 4 + 3	46 %	47 %	17 %	12 %

TB MR-targeted biopsy, *SB* systematic biopsy, *BN* biopsy naive, *PNB* prior negative biopsy, *AS* active surveillance, *CCL* cancer-core length, *GS* Gleason score

[a]All studies used T2-weighted, diffusion-weighted, and dynamic contrast-enhanced magnetic resonance imaging sequences, with any additional sequences listed above

Among Men with No Previous Biopsy

The use of MRI among men with no previous biopsy has been studied but currently its cost-effectiveness and true benefit are yet to be determined by larger randomized studies, as such its use is currently investigational. Haffner et al. reported a seminal series of 555 consecutive patients undergoing pre-biopsy MRI followed by systematic biopsy and visual estimation biopsy of MRI abnormalities. The overall cancer detection rate (CDR) was 54 % using extended systematic biopsy and 63 % amongst the 351 cases with an abnormal MRI [2]. Although systematic biopsy detected 66 more cases of cancer, 53 were deemed clinically insignificant. The MRI-targeted approach detected more high-grade cases and better quantified the cancer through increased cancer length per biopsy core. Delongchamps et al. also examined the use of pre-biopsy mpMRI in 391 consecutive patients and reported CDR of 41 % using systematic biopsy and 43 % using cognitive or fusion-targeted biopsy [45]. Targeted biopsy was significantly better at detecting high Gleason score (>3 + 3) cancer, missing only 2/63 (3 %) high-grade cancers detected by systematic biopsy while detecting an additional 17 high-grade cancers missed by systematic biopsy and avoiding detection of 39 Gleason 6 cancers [45]. Among 1448 men with pre-biopsy DW-MRI prior to initial biopsy, Watanabe et al. reported a CDR of 70.1 % in 890 patients with MRI lesions who underwent both targeted and systematic biopsy, compared to a CDR of only 13.1 % in 558 patients with no MRI lesions who only underwent systematic biopsy [46]. CDR was 90.1 % in 141 patients with anterior cancers found on MRI, an area easily missed with standard systematic biopsy [46]. A number of additional studies have demonstrated similar results (Table 8.1) [2, 47, 48].

Among Men with Previous Negative Biopsy

In a series of 438 consecutive patients with elevated PSA and at least one prior negative biopsy who underwent mpMRI, Hoeks et al. reported a CDR of 41 % (108/265) using in-bore targeted biopsy, with 87 % (94/108) of these cancers found to be clinically significant [49]. Vourganti et al. report on 195 patients with previous negative biopsy and suspicious mpMRI, finding a CDR of 37 % (73/195) using a combination of MRI-US fusion biopsy and systematic biopsy [50]. In addition to detecting nine additional high-grade cancers missed by systematic biopsy, fusion biopsy leads to pathological upgrading in 28/73 (38.4 %) patients [50]. Sonn et al. found a CDR of 34 % (36/105) in men with previous negative biopsy with 72 % (26/36) being clinically significant [24]. MRI-US fusion biopsy detected clinically significant cancer in 21/23 (91 %) men compared to only 15/28 (54 %) men with systematic biopsy. A highly suspicious MRI lesion was the most significant predictor of significant cancer on multivariate analysis [24]. Even in patients with up to four prior negative biopsies, Labanaris et al. found that among 170/260 (65 %) of patients with a suspicious MRI, PCa was detected on 96/170 (56 %) targeted

biopsies compared to only 30/170 (18 %) systematic biopsies [51]. A subgroup analysis of our institutional cohort demonstrated that among 172 men with prior negative biopsies and suspicious lesions on MRI, targeted biopsies missed no high-grade cancers, while detecting 15/31 (48 %) additional high-grade cancers missed by systematic biopsy. Additionally, the majority of cancers detected by systematic biopsy and missed or mischaracterized by targeted biopsy was found to be low volume and met clinical criteria for insignificant disease [52].

Among Men with Low-Risk Cancer

The performance of mpMRI and MRI-US fusion biopsy for monitoring patients with prostate cancer on active surveillance has yielded positive results which may improve risk stratification in these men [53, 54]. In a study of 388 consecutive patients with low-risk disease who underwent mpMRI and confirmatory visual estimation co-registration biopsy, Vargas et al. reported that 20 % (79/388) of patients were upgraded on confirmatory biopsy [55]. A 5-point MRI suspicion scale demonstrated excellent risk stratification, with a high sensitivity for upgrading on confirmatory biopsy (0.87–0.98) for a score of 5/5 [55]. In a study of 281 men, Ouzzane et al. showed mpMRI-targeted biopsy reclassified 10 % of patients who were eligible for active surveillance based on systematic biopsy [54]. In a recent study of 152 men meeting active surveillance criteria who underwent MRI-US fusions biopsy, Walton Diaz et al. determined that stable findings on mpMRI are associated with Gleason score stability and mpMRI appears promising as a useful aid for reducing the number of biopsies in the management of patients on active surveillance [56]. Additionally, Kim et al. demonstrated that among 287 men on active surveillance, high ADC values on DWI were strongly predictive of clinically insignificant, organ-confined disease [57]. MpMRI-based nomograms may further confirm eligibility for active surveillance and may decrease the number of repeat biopsies in patients on active surveillance by as much as 68 % [58].

Limitations of MRI-Targeted Biopsy

While MRI-targeted biopsy has the potential to overcome the limitations of standard TRUS-guided biopsy, it is not without several potential limitations itself. MRI-targeted biopsy incurs additional cost which remains to be justified through larger cohort studies. Imaging quality and quality of image-interpretation serves as a major barrier to widespread implementation in the community. Targeting methods are not purely defined and may still miss cancer. This targeting strategy may result in additional biopsies due to a false-positive MRI. Lastly, MRI-targeted biopsy may overestimate cancer risk, where further studies are needed to define the significance of pathology findings within the targeted biopsy.

Technique of MRI-Targeted Biopsy

Visual Estimation MR-Targeted TRUS Biopsy

Visual estimation allows adaptation of MRI-targeted biopsy in clinical practice without significant upfront cost, but carries a significant learning curve and lacks real-time feedback regarding accuracy. The effectiveness of visual estimation-targeted biopsy in detecting PCa varies between studies, likely reflecting inconsistencies in targeting precision, but generally visual estimation appears inferior to software co-registration [59, 60]. In a series of 351/555 (63 %) patients with a positive MRI, Haffner et al. detected clinically significant PCa in 45 % (248/555) of patients by systematic biopsy compared to 43 % (236/555) by visual estimation biopsy, but 53/66 cancers missed by targeted biopsy were clinically insignificant [2]. In contrast, Labanaris et al. reported CDR of 56 % by targeted visual estimation MRI-targeted biopsy alone but only 18 % by systematic biopsy alone in 170/260 (65 %) patients with a positive MRI [51]. Collectively, the currently published studies suggest improved accuracy and efficiency compared to systematic biopsy but also demonstrate that experience with visual estimation biopsy varies by investigator experience and likely, in part, due to variable practices in imaging approach.

Software Co-registered MRI-Targeted TRUS Biopsy

Software co-registration potentially overcomes the limitation of cognitive fusion through reproducible methods for identification of MRI lesions on ultrasound. A number of commercial platforms have become available [56]. These applications vary by method of co-registration (mechanical, electromagnetic, or real-time) and utilize different hardware platform for aligning the biopsy with the co-registered image. MRI/US fusion biopsy potentially has greater reproducibility due to less operator dependence and by providing real-time feedback of actual biopsied locations. Disadvantages include a high upfront cost for the software/device, dependence on the software for accuracy, and associated learning curve and operator training.

Table 8.3 summarizes reported outcomes of systematic biopsy vs. targeted biopsy using MRI/US fusion platforms evaluating clinically significant PCa. Siddiqui et al. recently reported that the combination of extended systematic and targeted biopsy using the Philips/PercuNav device resulted in diagnosing 30 % more high-risk cancers vs. standard biopsy (173 vs. 122 cases, $P<0.001$) and 17 % fewer low-risk cancers (213 vs. 258 cases, $P<0.001$) [4]. Sonn et al. report similar positive results using the Eigen/Artemis device, reporting a CDR of 53 % (90/171) with a higher percentage of positive cores (21 % vs. 7 %) and higher detection of Gleason ≥ 7 (38 % vs. 31 %) cancers using targeted biopsy [24]. Our institution experience with the Eigen/Artemis device has yielded similar results (Fig. 8.2) [5]. Patients with highly suspicious MRI lesions (5/5 grade) had a 94 % rate of cancer diagnosis compared to only 43 % in patients with low suspicious lesions (2/5 grade) [24]. High

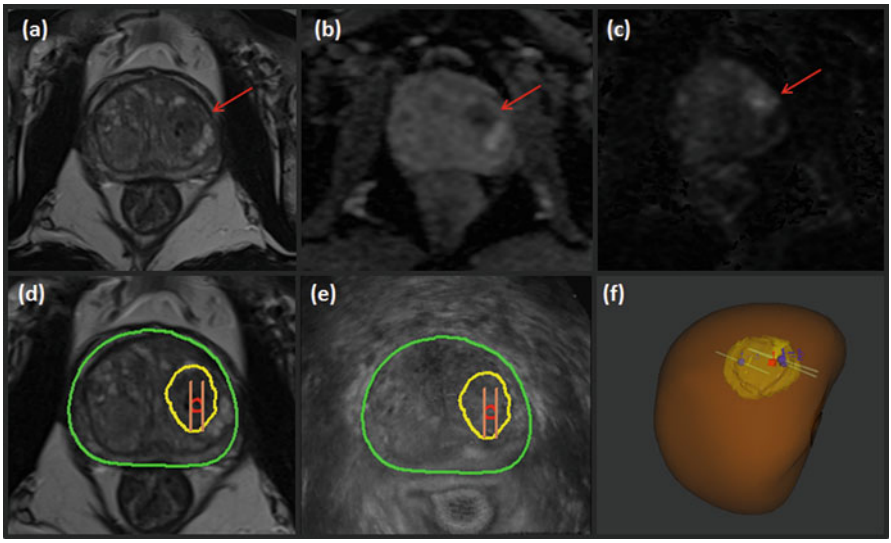

Fig. 8.2 Suspicious lesion visualized as (**a**) hypointense area on T2W image, (**b**) restricted diffusion with low ADC, and (**c**) high signal on diffusion-weighted image. Targeted biopsy workflow showing segmented prostate and lesion on (**d**) T2-weighted MRI, (**e**) transrectal ultrasound, and (**f**) 3D reconstruction of prostate and suspicious region

detection rates have also been demonstrated with transperineal MRI/US fusion biopsy. Kuru et al. reported a CDR of 58 % (200/347) (58 %) using the MedCom/BiopSee device, with a CDR of 82.6 % (86/104) in patients with highly suspicious lesions compared to only 15 % (14/94) in patients with a normal mpMRI [61].

In Bore MRI-Guided Biopsy

Hoeks et al. reported on 265 patients with suspicious lesions on mpMRI with prior negative TRUS biopsies that underwent transrectal in-bore MRGB, resulting in CDR of 41 % with 87 % of these detected cancers found to be clinically significant [49]. Multiple studies have corroborated this result, demonstrating that in-bore MRGB is a feasible diagnostic technique in patients with prior negative biopsy with a median detection rate of 42 %, significantly higher than reported detection rates for repeat systematic biopsy [62]. This in-bore biopsy strategy has the advantages of real-time feedback of needle placement, fewer sampled cores, and a low likelihood of missed target. It has the disadvantage of increased cost, use of scanner time (opportunity cost), and an inability to routinely sample the remaining gland. Additionally, in applying in bore MRI-guided biopsy, urologists are largely removed from the diagnostic pathway with concerning implications for the ultimate management of the disease.

Comparative Studies

While many studies compare targeted to systematic biopsy, only a few studies have compared the CDR between different targeted techniques. Recently, Cool and colleagues analyzed 225 simulated targeted biopsies by both visual estimation and MRI–ultrasound fusion and found MRI-targeted TRUS-guided prostate biopsy using cognitive registration appears to be inferior to MRI-TRUS fusion, with fewer than 50 % of clinically significant PCA lesions successfully sampled [60]. Wysock et al. prospectively compared MRI/US fusion biopsy using the Eigen/Artemis system vs. visual estimation targeting for 125 consecutive men with suspicious regions on pre-biopsy mpMRI and found that fusion targeting had improved accuracy for smaller MRI lesions and trended toward increased detection compared to visual targeting for all cancer (32.0 % vs. 26.7 %) as well as Gleason sum ≥ 7 cancers (20.3 % vs. 15.1 %) [59]. Delongchamps et al. reported that cognitive fusion was not significantly better than systematic random biopsies, while both software co-registration devices tested (Esaote/MyLabTMTwice and Koelis/Urostation) significantly increased CDR compared to systematic biopsies using conditional logistic regression analysis in a cohort of 391 patients [45]. Yet to be explored are the relationship of clinical factors such as prostate size, PSA, and location of MRI lesion on the accuracy of targeting by cognitive or co-registered approach. While more comparative studies examining the efficacy of different techniques are needed, it is possible that the decision for an institution or practice to utilize a particular type of MRI-targeted biopsy will be largely influenced by local factors such as cost, space, and operator experience with MRI interpretation. Recently through a consensus meeting, guidelines were published regarding conduct and standards in reporting MRI-targeted biopsy studies [63].

Conclusions

MpMRI represents a potential tool for addressing many of the limitations of contemporary systematic biopsy as MRI suspicion score correlated with significant disease. MpMRI appears to have a high negative predictive value, potentially reducing the need for a prostate biopsy in men with a normal MRI. However, there appears to be substantial variation in estimation of MRI tumor volume compared to pathological volume. Among men with no previous biopsy, targeted prostate biopsy using MRI guidance has the potential to reduce false negatives, improve risk classification, and contribute to reduction of repeat biopsies and over-detection. Among men with previous negative biopsy, but persistent suspicion, it has the potential to increase cancer detection and reduce further repeat biopsy. Among men with cancer contemplating surveillance, MR-targeted biopsy potentially improves risk stratification and reduces the need for repetitive biopsy. The optimal method for MR-targeted biopsy is not yet established, but emerging methods of co-registration

may offer wider accessibility to the approach. Further comparative studies to standard of practice and evaluation of cost-effectiveness are warranted prior to consideration of wide adoption.

Acknowledgement Neil Mendhiratta and Samir S. Taneja are supported by the Joseph and Diane Steinberg Charitable Trust.

References

1. Bjurlin MA, Meng X, Le Nobin J, et al. Optimization of prostate biopsy: the role of magnetic resonance imaging targeted biopsy in detection, localization and risk assessment. J Urol. 2014;192(3):648–58.
2. Haffner J, Lemaitre L, Puech P, et al. Role of magnetic resonance imaging before initial biopsy: comparison of magnetic resonance imaging-targeted and systematic biopsy for significant prostate cancer detection. BJU Int. 2011;108(8 Pt 2):E171–8.
3. Bjurlin MA, Carter HB, Schellhammer P, et al. Optimization of initial prostate biopsy in clinical practice: sampling, labeling and specimen processing. J Urol. 2013;189(6):2039–46.
4. Siddiqui MM, Rais-Bahrami S, Turkbey B, et al. Comparison of MR/ultrasound fusion-guided biopsy with ultrasound-guided biopsy for the diagnosis of prostate cancer. JAMA. 2015;313(4):390–7.
5. Meng X, Rosenkrantz AB, Mendhiratta N et al. Relationship of pre-biopsy multiparametric MRI and biopsy indication with MRI-US fusion-targeted prostate biopsy outcomes. Paper presented at: American Urological Association Annual Meeting, New Orleans, LA, 17 May 2015.
6. Hricak H, Dooms GC, McNeal JE, et al. MR imaging of the prostate gland: normal anatomy. AJR Am J Roentgenol. 1987;148(1):51–8.
7. Wang L, Mazaheri Y, Zhang J, Ishill NM, Kuroiwa K, Hricak H. Assessment of biologic aggressiveness of prostate cancer: correlation of MR signal intensity with Gleason grade after radical prostatectomy. Radiology. 2008;246(1):168–76.
8. Akin O, Sala E, Moskowitz CS, et al. Transition zone prostate cancers: features, detection, localization, and staging at endorectal MR imaging. Radiology. 2006;239(3):784–92.
9. Kim CK, Park BK, Kim B. High-b-value diffusion-weighted imaging at 3 T to detect prostate cancer: comparisons between b values of 1,000 and 2,000 s/mm^2. AJR Am J Roentgenol. 2010;194(1):W33–7.
10. Katahira K, Takahara T, Kwee TC, et al. Ultra-high-b-value diffusion-weighted MR imaging for the detection of prostate cancer: evaluation in 201 cases with histopathological correlation. Eur Radiol. 2011;21(1):188–96.
11. Mazaheri Y, Vargas HA, Akin O, Goldman DA, Hricak H. Reducing the influence of b-value selection on diffusion-weighted imaging of the prostate: evaluation of a revised monoexponential model within a clinical setting. J Magn Reson Imaging. 2012;35(3):660–8.
12. Hambrock T, Hoeks C, Hulsbergen-van de Kaa C, et al. Prospective assessment of prostate cancer aggressiveness using 3-T diffusion-weighted magnetic resonance imaging-guided biopsies versus a systematic 10-core transrectal ultrasound prostate biopsy cohort. Eur Urol. 2012;61(1):177–84.
13. Turkbey B, Shah VP, Pang Y, et al. Is apparent diffusion coefficient associated with clinical risk scores for prostate cancers that are visible on 3-T MR images? Radiology. 2011;258(2):488–95.
14. Parker GJ, Tofts PS. Pharmacokinetic analysis of neoplasms using contrast-enhanced dynamic magnetic resonance imaging. Top Magn Reson Imaging. 1999;10(2):130–42.
15. Turkbey B, Choyke PL. Multiparametric MRI and prostate cancer diagnosis and risk stratification. Curr Opin Urol. 2012;22(4):310–5.
16. Villers A, Puech P, Mouton D, Leroy X, Ballereau C, Lemaitre L. Dynamic contrast enhanced, pelvic phased array magnetic resonance imaging of localized prostate cancer for predicting

tumor volume: correlation with radical prostatectomy findings. J Urol. 2006;176(6 Pt 1): 2432–7.
17. Delongchamps NB, Rouanne M, Flam T, et al. Multiparametric magnetic resonance imaging for the detection and localization of prostate cancer: combination of T2-weighted, dynamic contrast-enhanced and diffusion-weighted imaging. BJU Int. 2011;107(9):1411–8.
18. Yoshizako T, Wada A, Hayashi T, et al. Usefulness of diffusion-weighted imaging and dynamic contrast-enhanced magnetic resonance imaging in the diagnosis of prostate transition-zone cancer. Acta Radiol. 2008;49(10):1207–13.
19. Jung JA, Coakley FV, Vigneron DB, et al. Prostate depiction at endorectal MR spectroscopic imaging: investigation of a standardized evaluation system. Radiology. 2004;233(3):701–8.
20. Barentsz JO, Richenberg J, Clements R, et al. ESUR prostate MR guidelines 2012. Eur Radiol. 2012;22(4):746–57.
21. Rosenkrantz AB, Kim S, Lim RP, et al. Prostate cancer localization using multiparametric MR imaging: comparison of Prostate Imaging Reporting and Data System (PI-RADS) and Likert scales. Radiology. 2013;269(2):482–92.
22. Rosenkrantz AB, Lim RP, Haghighi M, Somberg MB, Babb JS, Taneja SS. Comparison of interreader reproducibility of the prostate imaging reporting and data system and likert scales for evaluation of multiparametric prostate MRI. AJR Am J Roentgenol. 2013;201(4):W612–8.
23. Radiology ACo. MR Prostate Imaging Reporting and Data System version 2.0. 2015. http://www.acr.org/Quality-Safety/Resources/PIRADS/
24. Sonn GA, Natarajan S, Margolis DJA, et al. Targeted biopsy in the detection of prostate cancer using an office based magnetic resonance ultrasound fusion device. J Urol. 2013;189(1):86–91.
25. Yerram NK, Volkin D, Turkbey B, et al. Low suspicion lesions on multiparametric magnetic resonance imaging predict for the absence of high-risk prostate cancer. BJU Int. 2012;110(11 Pt B):E783–8.
26. Kumar R, Nayyar R, Kumar V, et al. Potential of magnetic resonance spectroscopic imaging in predicting absence of prostate cancer in men with serum prostate-specific antigen between 4 and 10 ng/ml: a follow-up study. Urology. 2008;72(4):859–63.
27. Squillaci E, Manenti G, Mancino S, et al. MR spectroscopy of prostate cancer. Initial clinical experience. J Exp Clin Cancer Res. 2005;24(4):523–30.
28. Manenti G, Squillaci E, Carlani M, Mancino S, Di Roma M, Simonetti G. Magnetic resonance imaging of the prostate with spectroscopic imaging using a surface coil. Initial clinical experience. Radiol Med. 2006;111(1):22–32.
29. Wysock JS, Zattoni F, Meng X et al. Predictive value of negative 3T multiparametric prostate MRI on 12 core biopsy results. Submitted.
30. Pokorny MR, de Rooij M, Duncan E, et al. Prospective study of diagnostic accuracy comparing prostate cancer detection by transrectal ultrasound-guided biopsy versus magnetic resonance (MR) imaging with subsequent MR-guided biopsy in men without previous prostate biopsies. Eur Urol. 2014;66(1):22–9.
31. Itatani R, Namimoto T, Atsuji S, et al. Negative predictive value of multiparametric MRI for prostate cancer detection: outcome of 5-year follow-up in men with negative findings on initial MRI studies. Eur J Radiol. 2014;83(10):1740–5.
32. Villeirs GM, De Meerleer GO, De Visschere PJ, Fonteyne VH, Verbaeys AC, Oosterlinck W. Combined magnetic resonance imaging and spectroscopy in the assessment of high grade prostate carcinoma in patients with elevated PSA: a single-institution experience of 356 patients. Eur J Radiol. 2011;77(2):340–5.
33. Hoeks CM, Barentsz JO, Hambrock T, et al. Prostate cancer: multiparametric MR imaging for detection, localization, and staging. Radiology. 2011;261(1):46–66.
34. Kim CK, Park BK, Kim B. Localization of prostate cancer using 3T MRI: comparison of T2-weighted and dynamic contrast-enhanced imaging. J Comput Assist Tomogr. 2006;30(1): 7–11.
35. Nakashima J, Tanimoto A, Imai Y, et al. Endorectal MRI for prediction of tumor site, tumor size, and local extension of prostate cancer. Urology. 2004;64(1):101–5.

36. Rud E, Klotz D, Rennesund K, et al. Detection of the index tumour and tumour volume in prostate cancer using T2-weighted and diffusion-weighted magnetic resonance imaging (MRI) alone. BJU Int. 2014;114(6b):E32–42.
37. Turkbey B, Mani H, Aras O, et al. Correlation of magnetic resonance imaging tumor volume with histopathology. J Urol. 2012;188(4):1157–63.
38. Isebaert S, Van den Bergh L, Haustermans K, et al. Multiparametric MRI for prostate cancer localization in correlation to whole-mount histopathology. J Magn Reson Imaging. 2013;37(6): 1392–401.
39. Baco E, Ukimura O, Rud E, et al. Magnetic resonance imaging-transectal ultrasound image-fusion biopsies accurately characterize the index tumor: correlation with step-sectioned radical prostatectomy specimens in 135 patients. Eur Urol. 2015;67:787–94.
40. Le Nobin J, Orczyk C, Deng FM, et al. Prostate tumour volumes: evaluation of the agreement between magnetic resonance imaging and histology using novel co-registration software. BJU Int. 2014;114(6b):E105–12.
41. Cornud F, Khoury G, Bouazza N, et al. Tumor target volume for focal therapy of prostate cancer-does multiparametric magnetic resonance imaging allow for a reliable estimation? J Urol. 2014;191(5):1272–9.
42. Anwar M, Westphalen AC, Jung AJ, et al. Role of endorectal MR imaging and MR spectroscopic imaging in defining treatable intraprostatic tumor foci in prostate cancer: quantitative analysis of imaging contour compared to whole-mount histopathology. Radiother Oncol. 2014;110(2):303–8.
43. Le Nobin J, Rosenkrantz AB, Villers A et al. Image guided focal therapy of MRI-visible prostate cancer: defining a 3D treatment margin based on MRI-histology co-registration analysis. J Urol. 2015. doi: 10.1016/j.juro.2015.02.080.
44. Puech P, Rouviere O, Renard-Penna R, et al. Prostate cancer diagnosis: multiparametric MR-targeted biopsy with cognitive and transrectal US-MR fusion guidance versus systematic biopsy—prospective multicenter study. Radiology. 2013;268:461–9.
45. Delongchamps NB, Peyromaure M, Schull A, et al. Prebiopsy magnetic resonance imaging and prostate cancer detection: comparison of random and targeted biopsies. J Urol. 2013;189(2):493–9.
46. Watanabe Y, Terai A, Araki T, et al. Detection and localization of prostate cancer with the targeted biopsy strategy based on ADC map: a prospective large-scale cohort study. J Magn Reson Imaging. 2012;35(6):1414–21.
47. Mozer P, Rouprêt M, Le Cossec C, et al. First round of targeted biopsies using magnetic resonance imaging/ultrasonography fusion compared with conventional transrectal ultrasonography-guided biopsies for the diagnosis of localised prostate cancer. BJU Int. 2015;115(1):50–7.
48. Numao N, Yoshida S, Komai Y, et al. Usefulness of pre-biopsy multiparametric magnetic resonance imaging and clinical variables to reduce initial prostate biopsy in men with suspected clinically localized prostate cancer. J Urol. 2013;190(2):502–8.
49. Hoeks CM, Schouten MG, Bomers JG, et al. Three-Tesla magnetic resonance-guided prostate biopsy in men with increased prostate-specific antigen and repeated, negative, random, systematic, transrectal ultrasound biopsies: detection of clinically significant prostate cancers. Eur Urol. 2012;62(5):902–9.
50. Vourganti S, Rastinehad A, Yerram NK, et al. Multiparametric magnetic resonance imaging and ultrasound fusion biopsy detect prostate cancer in patients with prior negative transrectal ultrasound biopsies. J Urol. 2012;188(6):2152–7.
51. Labanaris AP, Engelhard K, Zugor V, Nutzel R, Kuhn R. Prostate cancer detection using an extended prostate biopsy schema in combination with additional targeted cores from suspicious images in conventional and functional endorectal magnetic resonance imaging of the prostate. Prostate Cancer Prostatic Dis. 2010;13(1):65–70.
52. Mendhiratta N, Meng X, Rosenkrantz AB, et al. Pre-biopsy MRI and MRI-ultrasound fusion-targeted prostate biopsy in men with previous negative biopsies: improved cancer detection and risk stratification. Paper presented at American Urological Association Annual Meeting, New Orleans, LA, 17 May 2015.

53. Turkbey B, Mani H, Aras O, et al. Prostate cancer: can multiparametric MR imaging help identify patients who are candidates for active surveillance? Radiology. 2013;268(1):144–52.
54. Ouzzane A, Renard-Penna R, Marliere F, et al. MRI-targeted biopsy improves selection of patients considered for active surveillance for clinically low-risk prostate cancer based on systematic biopsies. J Urol. 2015. doi: 10.1016/j.juro.2015.02.2938.
55. Vargas HA, Akin O, Afaq A, et al. Magnetic resonance imaging for predicting prostate biopsy findings in patients considered for active surveillance of clinically low risk prostate cancer. J Urol. 2012;188(5):1732–8.
56. Logan JK, Rais-Bahrami S, Turkbey B, et al. Current status of magnetic resonance imaging (MRI) and ultrasonography fusion software platforms for guidance of prostate biopsies. BJU Int. 2014;114(5):641–52.
57. Kim TH, Jeong JY, Lee SW, et al. Diffusion-weighted magnetic resonance imaging for prediction of insignificant prostate cancer in potential candidates for active surveillance. Eur Radiol. 2015;25:1786–92.
58. Siddiqui MM, Truong H, Rais-Bahrami S, et al. Clinical implications of a multiparametric MRI based nomogram applied to prostate cancer active surveillance. J Urol. 2015;193:1943–9.
59. Wysock JS, Rosenkrantz AB, Huang WC, et al. A prospective, blinded comparison of magnetic resonance (MR) imaging-ultrasound fusion and visual estimation in the performance of MR-targeted prostate biopsy: the PROFUS Trial. Eur Urol. 2014;66(2):343–51.
60. Cool DW, Zhang X, Romagnoli C, Izawa JI, Romano WM, Fenster A. Evaluation of MRI-TRUS fusion versus cognitive registration accuracy for MRI-targeted, TRUS-guided prostate biopsy. AJR Am J Roentgenol. 2015;204(1):83–91.
61. Kuru TH, Roethke MC, Seidenader J, et al. Critical evaluation of MRI-targeted TRUS-guided transperineal fusion biopsy for detection of prostate cancer. J Urol. 2013;190(4):1380–6.
62. Overduin CG, Futterer JJ, Barentsz JO. MRI-guided biopsy for prostate cancer detection: a systematic review of current clinical results. Curr Urol Rep. 2013;14(3):209–13.
63. Moore CM, Kasivisvanathan V, Eggener S, et al. Standards of reporting for MRI-targeted biopsy studies (START) of the prostate: recommendations from an International Working Group. Eur Urol. 2013;64(4):544–52.
64. Fiard G, Hohn N, Descotes JL, Rambeaud JJ, Troccaz J, Long JA. Targeted MRI-guided prostate biopsies for the detection of prostate cancer: initial clinical experience with real-time 3-dimensional transrectal ultrasound guidance and magnetic resonance/transrectal ultrasound image fusion. Urology. 2013;81(6):1372–8.
65. Rastinehad AR, Turkbey B, Salami SS, et al. Improving detection of clinically significant prostate cancer: magnetic resonance imaging/transrectal ultrasound fusion guided prostate biopsy. J Urol. 2014;191(6):1749–54.
66. Sonn GA, Chang E, Natarajan S, et al. Value of targeted prostate biopsy using magnetic resonance-ultrasound fusion in men with prior negative biopsy and elevated prostate-specific antigen. Eur Urol. 2014;65(4):809–15.